applied sciences

MDPI

*Article*

# Hydration, Reactivity and Durability Performance of Low-Grade Calcined Clay-Silica Fume Hybrid Mortar

**Kwabena Boakye and Morteza Khorami ***

School of Energy, Construction & Environment, Faculty of Engineering & Computing, Coventry University, Coventry CV1 5FB, UK; boakyek4@uni.coventry.ac.uk
* Correspondence: morteza.khorami@coventry.ac.uk

**Abstract:** Low-grade calcined clay, due to its low cost, availability and low temperature calcination, has been gaining attention in recent times as a supplementary cementitious material (SCM) in the manufacture of revolutionary building materials to improve the fresh and hardened properties of concrete. Silica fume, on the other hand, has been used, over the years, to improve the performance of concrete due to its reduced porosity and improved transition zone quality. In spite of the individual contribution of these two pozzolans to the strength and durability of concrete, there is a knowledge gap in the properties of ternary blended mixes utilizing calcined clay and silica fume. In this study, the synergistic effect of calcined clay and silica fume on the fresh and hardened properties of cementitious mortar have been investigated. The two pozzolans were used to partially substitute Portland cement to form a ternary blended composite binder having, at a maximum, a replacement of 30% by weight and a varying content of calcined clay and silica fume. The influence of the binary and ternary blended mixes on hydration, pozzolanic reactivity and the mechanical and durability properties of mortar was studied. From the results, partial replacement of cement with 30% calcined clay and silica fume caused significant reductions in the portlandite content of the two hydrated pastes at all curing ages. Drying shrinkage was found to be less severe in the control mortar than the blended cement mixes. Compared to the blended cement specimens, the control suffered the most weight (13.3%) and strength (10%) losses, as indicated by the sulphate resistance test.

**Keywords:** calcined clay; drying shrinkage; sulphate resistance; pozzolanic reactivity; silica fume; ternary blends; freeze and thaw; durability



**Citation:** Boakye, K.; Khorami, M. Hydration, Reactivity and Durability Performance of Low-Grade Calcined Clay-Silica Fume Hybrid Mortar. *Appl. Sci.* **2023**, *13*, 11906. https://doi.org/10.3390/app132111906

Academic Editors: Carlos Thomas, Jose A. Sainz-Aja and Pablo Tamayo

Received: 16 October 2023
Revised: 28 October 2023
Accepted: 30 October 2023
Published: 31 October 2023



## 1. Introduction

Partial substitution of Portland cement with supplementary cementitious materials (SCMs) is a common approach in the reduction of carbon dioxide linked to the manufacture of clinker. The increased demand for SCMs, however, cannot be satisfied just with the conventional supplementary cementitious materials (SCM), including fly ashes, metakaolin, silica fume and granulated blast furnace slags (GGBS) [1]. This is made even more apparent by the possibility that the supply of these industrial by-products (mostly used as SCM) could decline drastically in the coming years [2].

As a result, low-grade calcined clay has been gaining attention in recent times as an SCM in the manufacture of revolutionary building materials to improve the fresh and hardened properties of concrete [3–5]. This is primarily due to its low cost, availability, low temperature calcination and easy grinding to achieve a higher surface area [6]. However, in comparison to other kaolinitic clays, low-grade clays have relatively minimal amounts of kaolinite, making its reactivity lower as compared to high purity clays [7]. That notwithstanding, some researchers [8–11] have reported on improved mechanical and durability characteristics when partially substituting with ordinary Portland cement in concrete. In contrast to the decarbonization of limestone during the production of Portland cement clinkers, the calcination of clays occurs at lower temperatures (500 and 850 °C) and typically

does not entail the emission of carbon dioxide. So, compared to the manufacturing of Portland clinkers, the production of calcined clays requires less energy and emits significantly less carbon dioxide.

To improve the performance of concrete, silica fume (SF) has historically been utilised more frequently [12–14]. Because of its reduced porosity and improved transition zone quality, SF, which must have a silica concentration of at least 85%, has been known to improve both strength and durability [15,16]. However, since silica fume is a waste product from the silicon industry, its cost and availability are greatly influenced by its proximity to raw material source. Additionally, because the particles are ultrafine, they have a large specific surface area, necessitating the use of water-reducing admixtures to improve workability [1].

Calcined clay is mainly aluminosiliceous, whereas silica fume is only a siliceous material. When calcined clay and silica fume react with the $Ca(OH)_2$ that is released during cement hydration, a gel is formed that is used to improve the binding properties of the solid components of the concrete mix. Calcium aluminate hydrate (C-A-H) and calcium silicate hydrate (C-S-H) are both components of the gel generated in calcined clay–cement reactions, whereas C-S-H is the major component of the gel produced in silica fume–cement reactions [17]. The effectiveness of calcined clay and silica fume when used alone in concrete have been thoroughly researched and reported [18–21]. Calcined clay typically has a higher workability than silica fume, but the impacts of calcined clay and silica fume on strength and durability depend on their pozzolanic reactivity and fineness. When used separately, calcined clay and silica fume are both quite effective in improving compressive and tensile strengths as well as lowering porosity, chloride ingress and drying shrinkage [16,21].

Because calcined clay and silica fume both have a higher surface area than cement, they would fill the voids and eventually increase packing density, water demand and setting times. In a blend of calcined clay and silica fume, it is expected that the combined pozzolan particles would fill the voids within the cementitious system, improving the packing factor better than individual calcined clay and silica fume, thereby enhancing the performance of the cementitious material.

In spite of the individual contribution of calcined clay and silica fume to the strength and durability of concrete, there have been few investigations into ternary blended mixes prepared with aluminosilicates and silica fume. Chu and Kwan [17] studied the influence of metakaolin and silica fume on the properties of mortar and reported increased 7- and 28-days strength and workability. Morsy, Shebl and Rashad [22] investigated the effect of fire on the properties of ternary blended silica fume and metakaolin. Concrete containing 15% metakaolin and 15% silica fume immensely enhanced thermal shock resistance compared to the reference cement concrete. In studying how a combination of metakaolin and silica fume affect concrete, Srivastava et al. reported an optimum silica fume dosage of 6% and 15% of metakaolin to produce improved compressive strength properties. In filling the research gap, it is observed that there is little or no literature discussing the properties of ternary blended mortar prepared with calcined clay and silica fume. In this study, the synergistic effect of calcined clay and silica fume on the fresh and hardened properties of cementitious mortar including setting time, soundness, mortar flow, pozzolanic reactivity and mechanical and durability properties have been investigated. The results of this work are in reference to ordinary Portland cement and the optimum replacement discussed.

## 2. Materials and Methods

### 2.1. Materials

The materials used in this work are high strength ordinary Portland cement (CEM I 52.5 N) supplied by Hanson. The cement had a fineness of 410 $m^2/kg$. Powdered silica fume, with a median particle size of 32 μm and specific gravity of 2.42, was obtained from Elkem. The calcined clay pozzolan was prepared by burning a low-grade clay, with a kaolinite composition of 20%, at a temperature of 900 °C for 2 h and a heating rate of

10 °C/h. The clay was taken from the kiln after calcination and placed on a laboratory bench for 2 h to cool to an ambient temperature. The calcined clay was milled and sieved to a fineness of 75 µm. The particle size distribution of the starting raw materials is shown in Figure 1. The chemical compositions and XRD (X-ray diffraction) spectra of the cement, calcined clay and silica fume are presented in Table 1 and Figures 2 and 3, respectively.

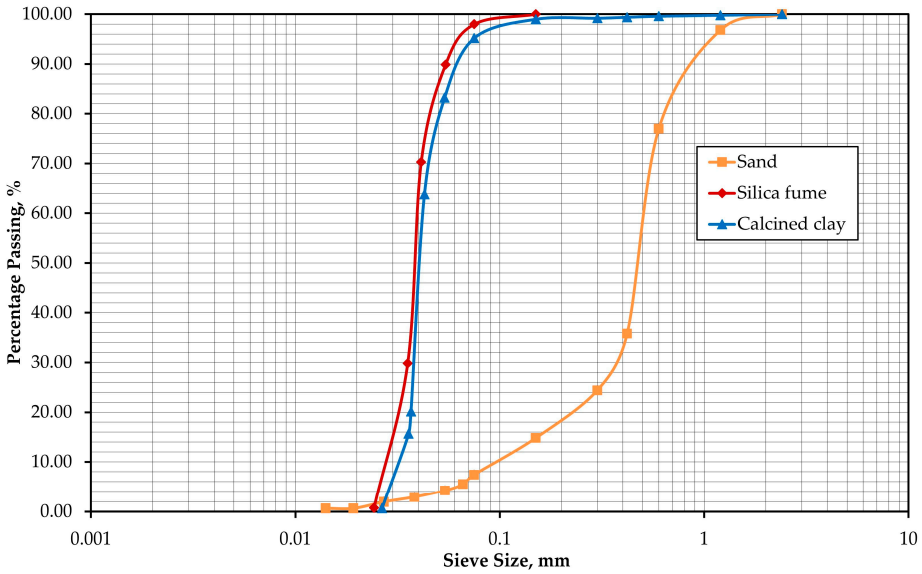


**Figure 1.** Particle size distribution of calcined clay, silica fume and sand.

**Table 1.** Chemical composition of raw materials.

| Composition, % | $SiO_2$ | $A1_2O_3$ | $Fe_2O_3$ | MgO | CaO | $Na_2O$ | $K_2O$ | MnO | $TiO_2$ | $P_2O_5$ | Cl | $SO_3$ | LOI |
|---|---|---|---|---|---|---|---|---|---|---|---|---|---|
| Calcined clay | 62.77 | 18.71 | 11.68 | 1.89 | 0.25 | 0.03 | 2.12 | 0.46 | 0.41 | 0.03 | - | 0.2 | 1.5 |
| Silica fume | 93.5 | - | 1.25 | 2.0 | 0.15 | - | 1.85 | - | - | - | - | 0.4 | 0.9 |
| Cement | 18.88 | 3.57 | 3.36 | 1.89 | 59.64 | 4.7 | 2.12 | 0.14 | 0.14 | 0.22 | 0.01 | 4.9 | 0.4 |

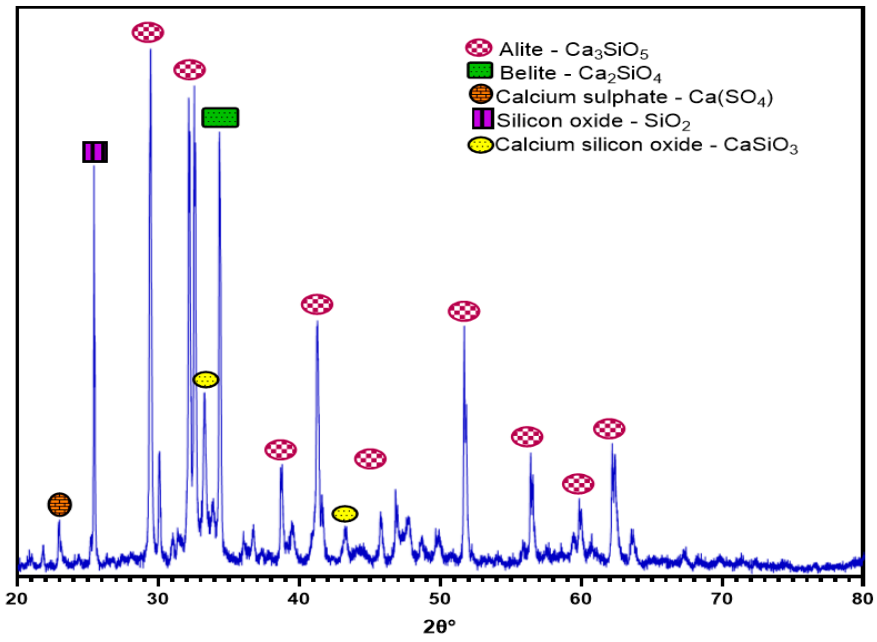


**Figure 2.** XRD of cement.

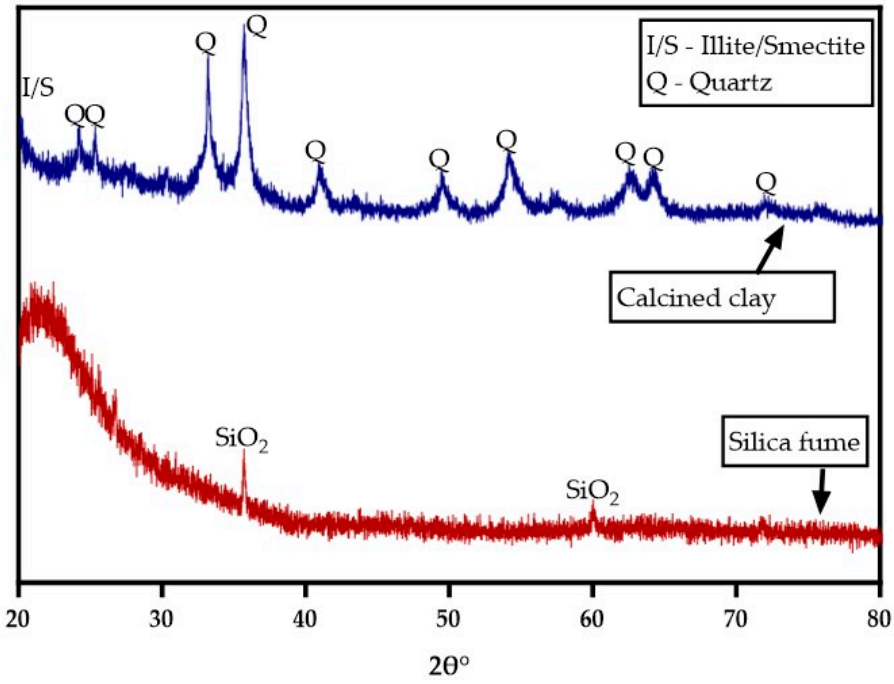


**Figure 3.** XRD of calcined clay and silica fume.

*2.2. Methods*

2.2.1. Blended Cement Preparation

The calcined clay and silica fume were used to partially substitute Portland cement to form a ternary blended composite binder with a maximum replacement of 30% by weight and a varying content of calcined clay and silica fume. Sample 1 comprised 100% cement, referred to as control. Sample 2 was made up of 20% calcined clay and 10% silica fume (20CC10SF), whereas Sample 3 contained a blend of 10% calcined clay and 20% silica fume (10CC20SF). Sample 4 constituted 15% apiece of calcined clay and silica fume. Samples 5 and 6 were made up of 30% silica fume and calcined clay, respectively (30SF and 30CC).

2.2.2. Testing Methods

X-ray diffraction (XRD) analyses of the powders and hydrated samples were conducted with a 3rd generation Malvern Panalytical Empyrean XRD Diffractometer. Thermogravimetric analysis (TGA) of the blended cement was conducted with the Perkin Elmer DSC 7 analyser. The samples, after curing for 3, 7, 28 and 91 days, were blended and placed in the TGA equipment. The temperature was raised up to 1000 °C at a heating rate of 20 °C/min. Nitrogen gas of 50 mL/min was flashed into the chamber to avoid carbonation. As recommended by Benkeser et al. [23], the blended cement samples were kept at 40 °C to allow for the removal of free water. The calcium hydroxide (CH) content of the samples was recorded after each curing period using equation 1 [23]. Calcium hydroxide content was calculated from the change in mass between temperatures 330 °C and 450 °C.

$$CH,\ \% = \left[ \left( Mass_{330^\circ C} - Mass_{450^\circ C} \right) \times \frac{4.113}{Mass_{40^\circ C}} \right] \times 100 \quad (1)$$

A thermometric TAM air conduction calorimeter was used to track the evolution of the hydration heat rate. Then, 5 g of the blended cement samples were mixed with distilled water and fixed inside the calorimeter at a working temperature of 20 °C. The attached computer automatically generated heat of hydration data continuously for up to 60 h.

Using ASTM C305 [24], mortar samples were prepared for the determination of compressive strength using a water-to-binder ratio of 0.5 and a sand-to-binder ratio of 3. Mortar flow was determined according to methods prescribed by ASTM C1437 [25]. The Vicat method,

specified by ASTM C191 [26], was used to determine the normal consistency and setting times of all the cement samples. Soundness was determined using the Le Chatelier's apparatus as prescribed by EN 196-3 [27].

A Frattini test was conducted with reference to BS EN 196-5:11 [28]. Then, 20 g of the samples were mixed with 100 mL deionised water in plastic vials, sealed tightly and kept at a temperature of 40 °C for 28 days. It was then filtered and titrated to determine the amount of $Ca^{2+}$ and $OH^-$. Determination of water sorptivity of the hardened blended cement paste was conducted utilising the sorptivity coefficient, as prescribed by ASTM C1585-13 [29]. Permeable porosity was determined using methods outlined by ASTM C642-13 [30].

With reference to IS:13311 (part-1), ultrasound pulse velocity was used to determine how dense the hardened blended cement mortar was. This is an indication of how long it takes for a pulse to move from one side of the hardened mortar to the other using the ultrasound pulse velocity transducers. Drying shrinkage was determined according to the ASTM C490-07 standard [31]. The first reading was taken after 3 h of curing and recorded as $L_0$. Final readings ($L_t$) were taken after 3, 7, 14, 28 and 91 days curing. The drying shrinkage of the samples were determined using Equation (2), where 250 (mm) is the effective length of the samples.

$$\varepsilon_t = \frac{L_t - L_0}{250} \quad (2)$$

For RCPT measurement, electrical current was allowed to pass through slices of mixed cement mortar samples for a total of six hours, using the ASTM C 1202 [32] RCPT technique. Sodium hydroxide and sodium chloride solutions were used to treat two slices of the same material, respectively. A potential difference of 60 V was preserved at the endpoints of the specimens. Samples were cured in water for 28 days before submerging in 5%-$Na_2SO_4$ solutions to conduct the sulphate resistance test. Following a 90-day standing period, the impact of the 5%-$Na_2SO_4$ solution on each subject's compressive strength and weight loss was assessed.

## 3. Results and Discussions

### 3.1. Water Demand, Setting Time and Soundness

Table 2 provides results for setting times, water demand and soundness. It is observed that each blended cement, depending on its material composition, impacted water demand and setting times differently. Blended cement containing 30% silica fume (30SF) and 30% calcined clay (30CC) recorded the least and highest water demand, respectively, which were also reflected in the setting time results. If cement retains its volume after setting it is mostly considered to be sound. The amount of free lime, MgO and $SO_3$ contained in cement is the main cause of its excessive expansion [33]. From Table 2, it can be seen that all results for the soundness test fell below the EN-196-3-specified maximum limit of 5.0 mm. This is due to the low MgO and $SO_3$ content in the blended cements [33,34]. The blended cements showed improved soundness as compared to the control.

**Table 2.** Normal consistency, setting time and soundness of blended cements.

| Sample | Control | 20CC10SF | 10CC20SF | 15CC15SF | 30SF | 30CC |
|---|---|---|---|---|---|---|
| Normal consistency, % | 28.7 | 32.4 | 31.4 | 30.8 | 27.5 | 33.1 |
| Initial setting time, min | 142 | 165 | 153 | 150 | 140 | 182 |
| Final setting time, min | 242 | 261 | 256 | 260 | 240 | 280 |
| Soundness, mm | 1.02 | 0.92 | 0.52 | 0.51 | 0.54 | 0.86 |

### 3.2. Mineralogical Studies

XRD patterns of 28-days hydrated blended cement pastes containing varying content of calcined clay and silica fume are shown in Figure 4. The XRD patterns, as identified by the ICDD database, reveal the presence of quartz, calcite, alite belite, calcium silicate hydrates and portlandite in both the reference and blended cement pastes. After 28 days

of hydration, the blended cement paste was found to have substantially smaller peaks, which is due to the reaction between the pozzolans and portlandite to create additional cementitious products like calcium silicate hydrates (C-S-H) [4,9].

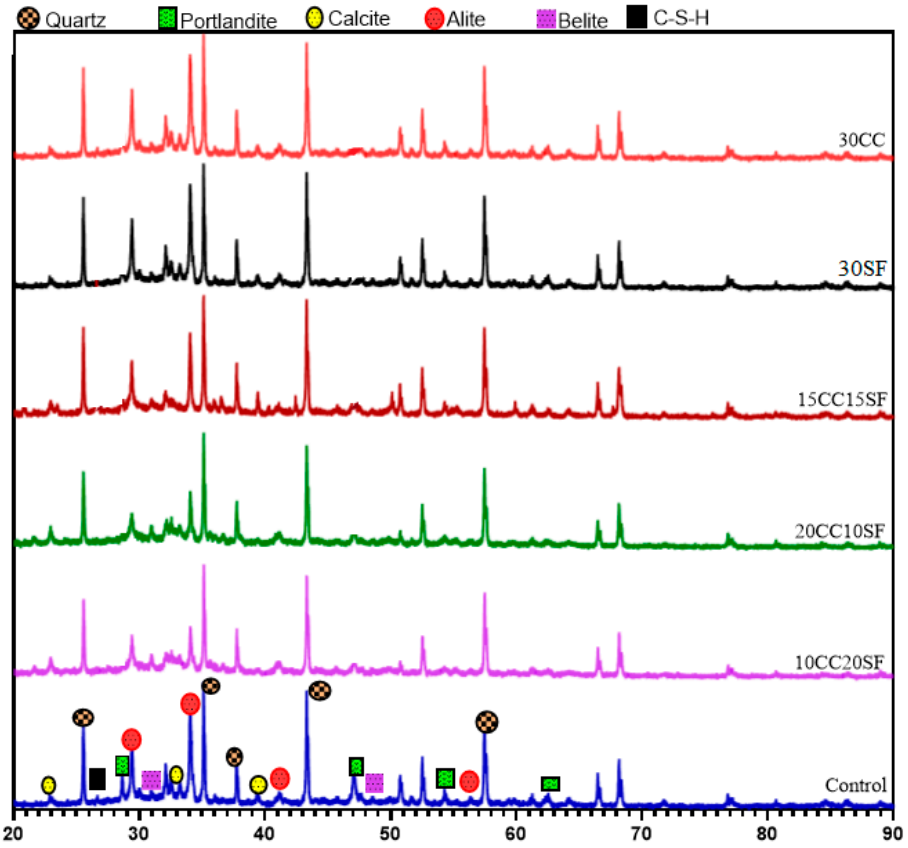


**Figure 4.** XRD pattern of hydrated blended cement mortars.

### *3.3. Pozzolanic Reactivity*

#### 3.3.1. Isothermal Calorimetry

Heat evolution was monitored to determine how blended cements influenced the kinetics of cement hydration using isothermal calorimetry. Figure 5a shows the heat flow of the blended cement pastes up to 60 h, and the amount of heat released throughout the period of hydration is shown in Figure 5b. In comparison to the control paste, calorimetry patterns for the blended cement pastes are anticipated to show higher peaks and acceleration during the hydration reaction. The results showed that the addition of the pozzolans clearly had an impact on the calorimetric properties of the blended cement pastes, especially on the primary peak. The incorporation of calcined clay and silica fume caused an increase in exothermic peak values and a decrease in peak times [35]. It can be seen that ternary mixed cements have substantially longer induction periods than the reference cement does, and that these periods lengthen as replacement levels rise. The long induction period is due to the low kaolinitic content of the calcined clay which slowed down the initial hydration process. However, the presence of $Al_2O_3$ and $SiO_2$, especially in the silica fume, hastens the reaction between $Ca(OH)_2$ from the cement to release heat and eventually enhance the hydration process [36]. Hydration in silica fume-rich pastes were found to be release lower amounts of heat as compared to pastes containing calcined clay. This impact becomes increasingly apparent as the pozzolan content rises, as evidenced in the compressive strength results reported in Section 3.5. Once more, it can be seen that the reference cement peak displays a bump, which often denotes the transformation of afwillite to monosulphate. This peak bump vanished in pastes containing pozzolans, caused by the effectiveness of pozzolanic reactivity [37]. This is in line with previous studies on the

hydration of ternary mixed cements with various pozzolan contents. It is also observed that, in comparison to the control, pastes containing calcined clay and silica fume reported lower exothermic peak values with shorter corresponding peak periods [21,38,39].

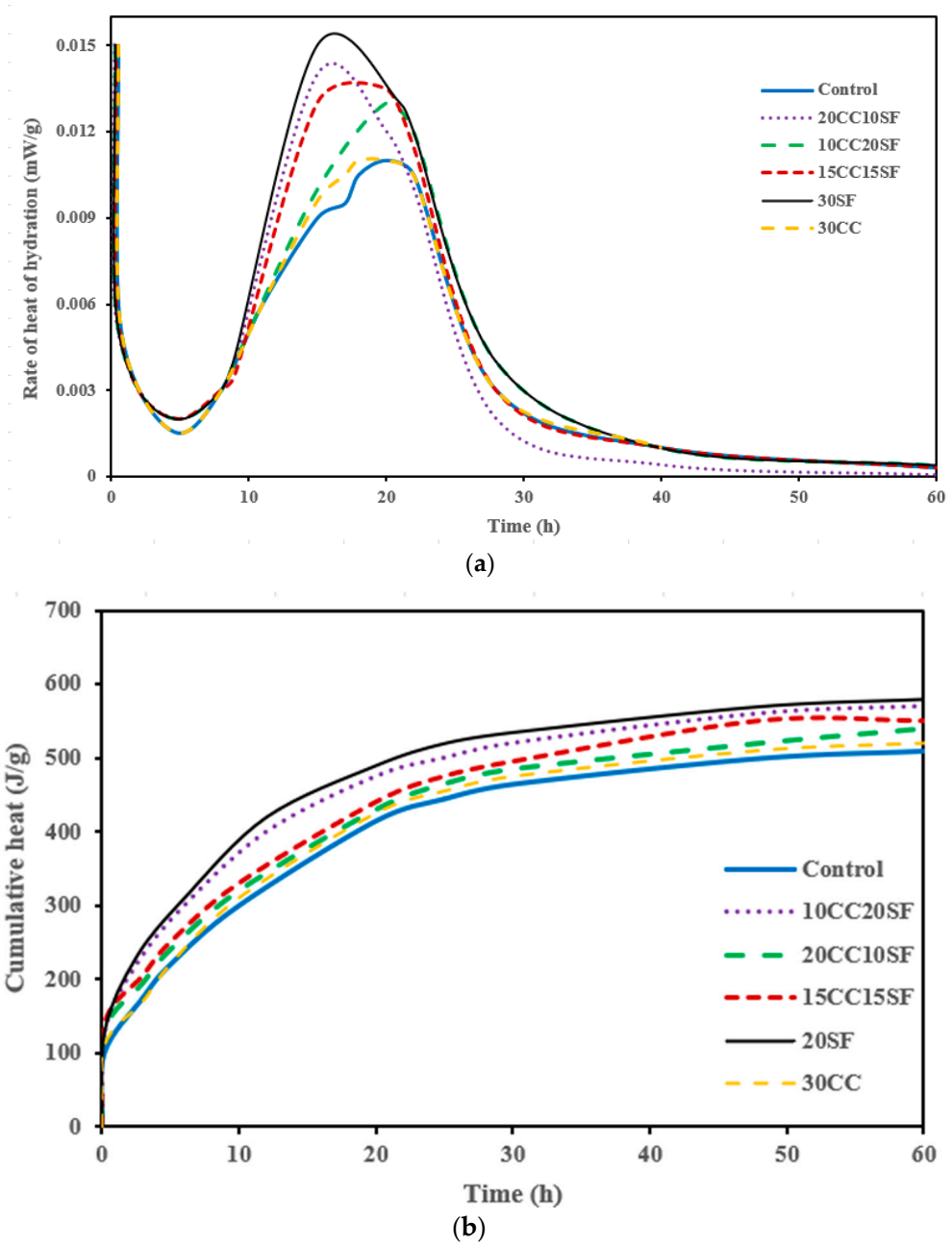


**Figure 5.** (**a**). Heat of evolution of blended cement. (**b**). Cumulative heat of blended cement.

### 3.3.2. Portlandite Consumption

Thermogravimetric analysis (TGA) was used to quantitatively evaluate the portlandite content (CH) in the blended cement pastes at 3, 7, 28 and 91 days, as a measure of pozzolanic reactivity. Generally, the higher the $Ca(OH)_2$ content remaining after hydration, the lower the reactivity of the material [23]. Figure 6 shows the formation of portlandite in the pastes with varying calcined clay and silica fume content. The reference cement paste was observed to exhibit a consistent rise in portlandite content up to 91 days of hydration. This was expected and in line with the results obtained by the heat of hydration test. The extent of hydration reaction and the amounts of tricalcium silicates and dicalcium silicates

account for this high portlandite content in the reference cement, which could influence mechanical strength development [40]. However, the portlandite content at early ages in the control sample was found to be lower than all the blended cement samples. This is because pozzolanic reactivity at early ages is known to proceed slowly [18,41]. This behaviour has also been reported by Wild and Khatib [42]. Partial replacement of cement with 30% calcined clay and silica fume caused significant reductions in the portlandite content of the two hydrated pastes at all curing ages. Between the two incorporated mineral admixtures, the paste prepared with only silica fume was found to contain less portlandite content at the end of the curing period. The portlandite content remaining in 30% silica fume pastes after 3, 7, 28 and 91 days hydration were 7.7%, 13.3%, 12.8% and 8.6%, respectively, less than that of the 30% calcined clay pastes. This is due to the lower kaolinite content of the clay which consequently affects pozzolanic reactivity, leaving some amounts of $Ca(OH)_2$ unreacted [43].

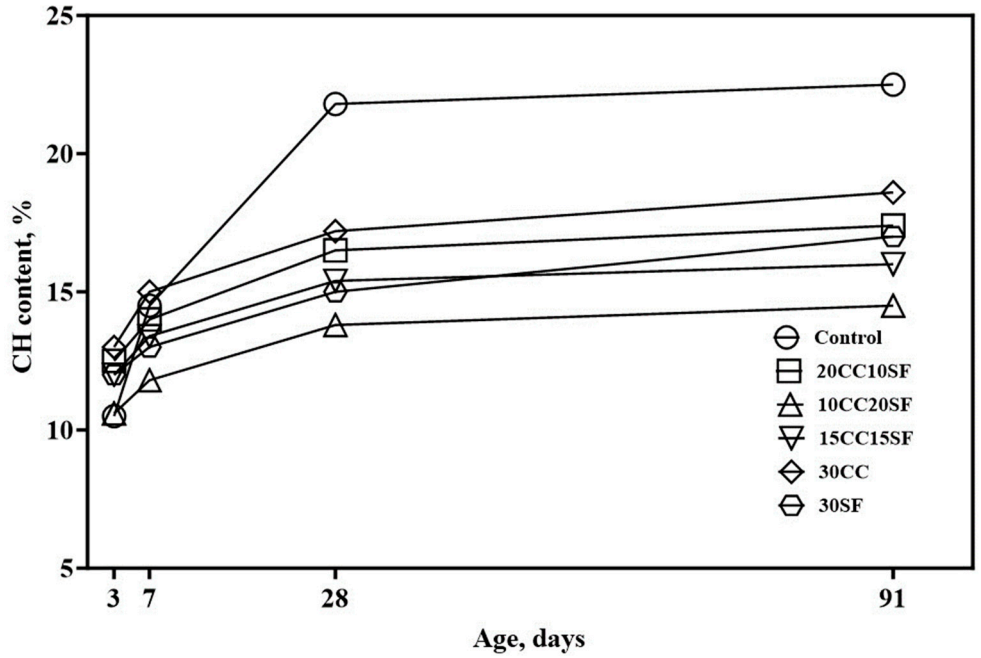


**Figure 6.** Portlandite content in hydrated calcined clay-silica fume blended cement pastes.

Pastes containing a ternary blend of silica fume and calcined clay showed a relatively higher degree of reactivity, resulting in lower portlandite content after hydrating for 91 days. Portlandite content ranged between 10.6% and 17.4%. It is noteworthy that pastes containing higher silica fume content recorded lower portlandite content. This is attributed to the high silica content and large surface area of the silica fume which lead to improved reactivity and the production of extra calcium silicate hydrate gels (C-S-H) [44]. Two factors are responsible for the overall decrease in portlandite content in the blended cement pastes. Firstly, the clinker component is significantly reduced due to pozzolan replacement, which invariably reduces the tricalcium silicate ($C_3S$) content, slowing down the hydration process. Secondly, the calcined clay and silica fume have high contents of amorphous silica which propels pozzolanic reaction and consumption of portlandite [45].

### 3.3.3. Frattini Test

The Frattini test is a widely recognized technique for evaluating pozzolanic reactivity of blended cements. After titration, the Frattini test results are presented as $Ca^{2+}$ and $OH^-$. A lime solubility curve is used to separate the pozzolanic area from the non-pozzolanic. A plot of the $OH^-$ against CaO in the form of $Ca^{2+}$ on the solubility curve gives an indication of the pozzolanic reactivity or otherwise of the blended cement. Table 3 presents the Frattini

test results data. Figure 7 shows the pozzolanic reactivity of the blended cement pastes at 28 days, as determined by Frattini test showing a plot of CaO against $OH^-$ [46]. Silica sand (inert material), known for its unreactivity, was used as a reference in determining the pozzolanic reactivity of the blended cements pastes. As demonstrated by the portlandite consumption in Figure 6, a specimen containing only calcined clay was found just below the lime solubility curve. This is an indication of pozzolanic reactivity, however small. The specimen containing 30% silica fume, on the other hand, was positioned far below the curve, outperforming all the blended cement pastes. This demonstrates the consumption of portlandite, confirming the material's pozzolanic properties. It is observed that specimens containing greater amounts of calcined clay showed relatively weaker reactivity due to lower kaolinite content. Silica sand is positioned within the over saturated region above the curve, signifying the absence of pozzolanic reactivity. This trend of reactivity is similar to observations reported by Boakye et al. [19].

**Table 3.** Frattini test results data.

| Sample | $OH^-$ (mmol/L) | CaO (mmol/L) |
|---|---|---|
| 30CC | 57.4 | 7.8 |
| 20CC10SF | 57.5 | 7.2 |
| 15CC15SF | 56.4 | 6.3 |
| 10CC20SF | 58.5 | 5.6 |
| 30SF | 59.3 | 4.8 |
| Silica sand | 58.6 | 10.4 |

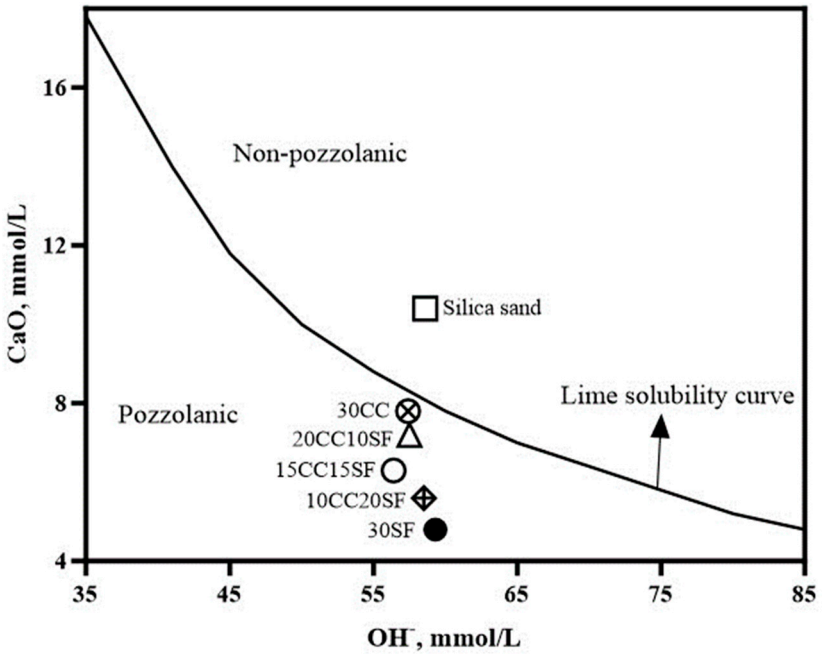


**Figure 7.** Pozzolanic reactivity by Frattini test.

### 3.4. Workability

The workability of the blended cement mortar containing varying silica fume and calcined clay content were determined by a measure of the relative mortar flow, as shown in Figure 8. The mortar flow of the control specimen (OPC) represents the 100% mortar flow mark on Figure 8. The workability of all the blended cement specimens were found to be less than the control specimens. With a constant water-to-cement ratio, mortar samples containing 30% silica fume (30SF) were observed to be the least workable among the blended cement mortars, obtaining a relative mortar flow of 54.7% compared to the control mortar. Samples marked 20CC10SF, 10CC20SF and 15CC15SF recorded relative mortar

flow of 80.7%, 60.3% and 78%, respectively. The mix containing 10% silica fume and 20% calcined clay (20%CC10SF) obtained the optimum workability. This is due to the smaller particle size of the silica fume which resulted in higher water demand to form a workable paste, as demonstrated in Table 2. The higher the silica fume content, the greater the water demand. This trend is consistent with results reported by earlier researchers [17,47,48].

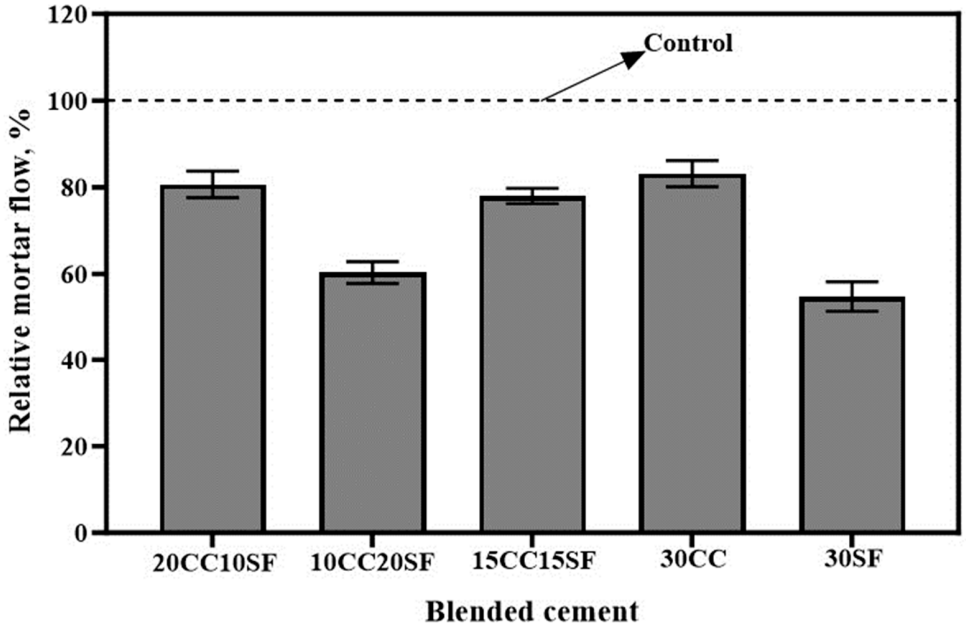


**Figure 8.** Relative mortar flow of blended cement mortar.

### *3.5. Mechanical Properties*

The relative compressive strength of the blended cement mortar is presented in Figure 9. The relative strength of the control mortar is represented by 100%. Compressive strength of all the blended cement mortar mixes trailed the control mortar at 3 and 7 days. SF-rich ternary blended mixes were observed to outperform the CC-rich mixes at early ages. This is attributed to the fact that calcined clay at early ages behaves as an inert material with little or no reactivity [41]. The reactivity of silica fume, on the other hand, has been reported to commence within the first 12 h of hydration [49]. It is also observed that the early-age strength (3 and 7 days) for 30CC and 30SF were lower as compared to the other mixes. This is due to the low and slow reactivity of pozzolanic materials at early ages, leading to lower strength development. Compressive strength, however, improved at 28 and 91 days, outperforming the control. At 28 days, apart from 30CC which fell short of the control mortar by 1%, all blended mixes recorded relative strengths greater than the control. Strengths obtained by 20CC10SF, 10CC20SF, 15CC15SF and 30SF were 1.3%, 16.7%, 13% and 9.1%, respectively, greater than the control. 10CC20SF obtained the highest relative strength at 28 days. This enhanced strength is due to the chemical interaction between $Ca(OH)_2$ from the cement hydration and glassy $SiO_2$ phases of the pozzolans to generate further cementitious compounds in the form of calcium silicate hydrates (C-S-H). The filler and lubricating effect of silica fume in cementitious matrices cause an improvement in the packing density and rheological characteristics of the resultant mortar, resulting in improved mechanical properties [50]. In addition, a lower kaolinite content of the calcined clay could be responsible for its low reactivity, even at 28 days, leading to a relatively lower strength development. All blended mixes outperformed the control mix when curing was extended to 91 days. Pozzolanic reactivity at 91 days improved significantly, even for CC-rich mortar mixes. This pattern of strength development is supported by the results obtained for the pozzolanic reactivity measurements in Section 3.3. This observation is consistent with results obtained by Chu and Kwan [17].

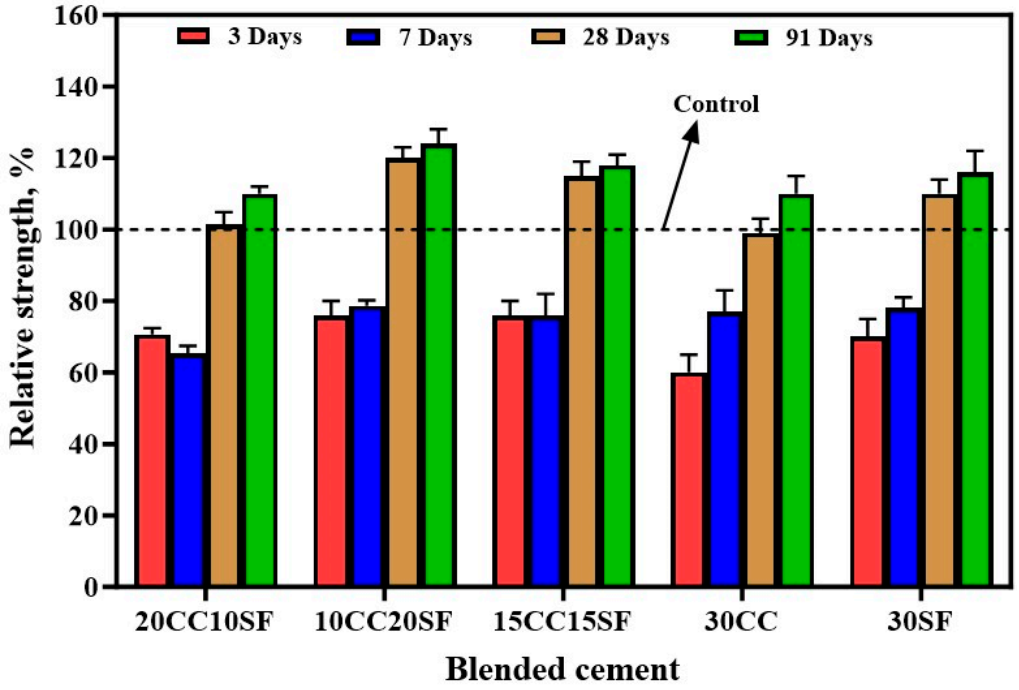


**Figure 9.** Relative compressive strength of blended cement mortar.

### *3.6. Durability*

#### 3.6.1. Sorptivity and Permeable Porosity

Figure 10 shows the sorptivity coefficient and permeable porosity results of the blended cement mixes prepared with varying content of calcined clay and silica fume. The sorptivity coefficient was reduced by 45% and 75.8% with the addition of 30% calcined clay and 30% silica fume, respectively. It is, therefore, clear that silica fume is superior to calcined clay in resisting water absorption. The sorptivity values recorded for 20CC10SF, 10CC20SF and 15CC15SF were 0.028 mm/s $^{0.5}$, 0.019 mm/s $^{0.5}$ and 0.026 mm/s $^{0.5}$, respectively. The higher the silica fume content, the lower the sorptivity coefficient. Permeable porosity results followed a similar trend. The sole inclusion of 30% calcined clay and silica fume caused reductions in permeable porosity by 73.4% and 87.1%, respectively. The control sample showed the least sorptivity coefficient and permeable porosity values. The presence of low-grade calcined clay in the mix could not significantly impact the sorptivity and porosity of the blended cement mixes. It appears that the properties of the silica fume overshadowed and affected the performance of calcined clay in the blended mixes. The results obtained are due to the particle size distribution of the silica fume which fill the voids within the cementitious matrix, refining the pores and leading to a decrease in sorptivity and porosity. Chen et al. [51] studied the influence of ternary blended silica fume and metakaolin on porosity and sorptivity and reported similar results.

#### 3.6.2. Freeze and Thaw Resistance

Figure 11 is a graphical presentation of the freeze–thaw resistance results of calcined clay-silica fume blended cement mortar mixes after 120 cycles. The control mix, before the freeze–thaw cycles recorded a compressive strength of 52 MPa, which steadily declined as the number of cycles increased. At the end of the 120 cycles, the control mix had retained about 62.9% of its strength. It is clear from the results that the control mix offered the least resistance to the cycles at all levels. This observation is consistent with earlier reports [52]. Generally, the freeze–thaw effect on blended cement mixes was observed to be marginal within the first 30 cycles and became more severe beyond 60 cycles. Even though all samples suffered a reduction in strength as a result of the freeze–thaw cycles, the blended cement samples, irrespective of pozzolan content and dosages, demonstrated a better

resistance compared to the control mix. Among the blended cement mixes, the specimen containing 30% silica fume (30SF) obtained the highest compressive strengths values.

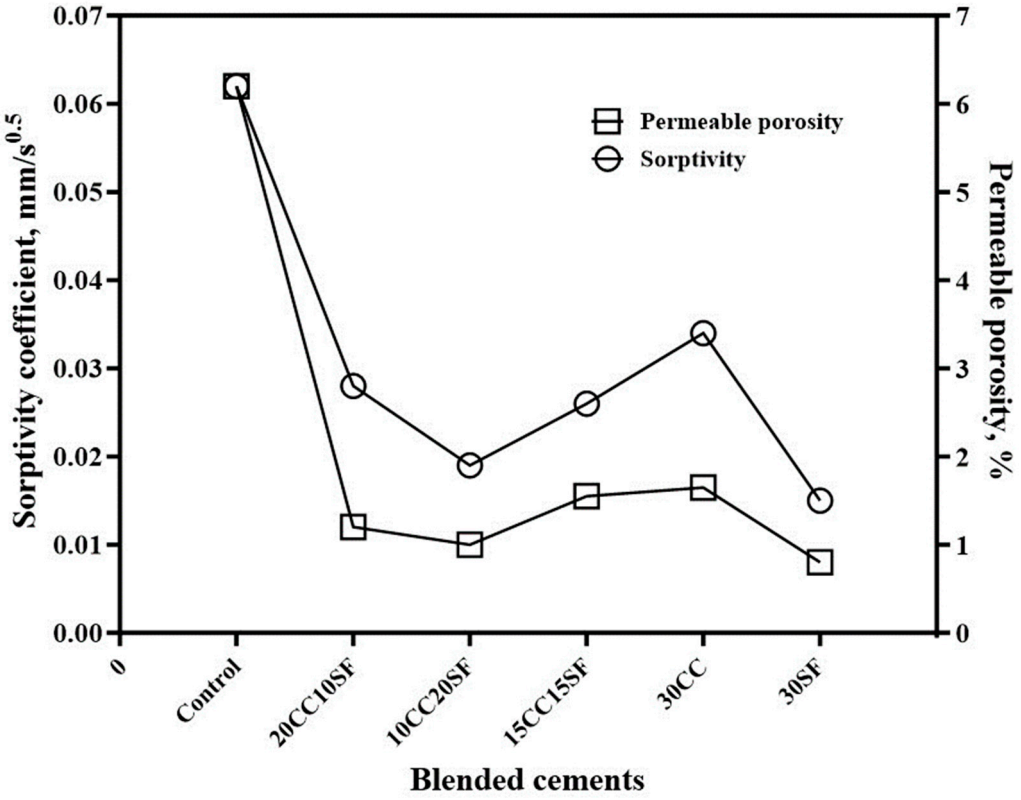


**Figure 10.** Sorptivity and permeability porosity of blended cements.

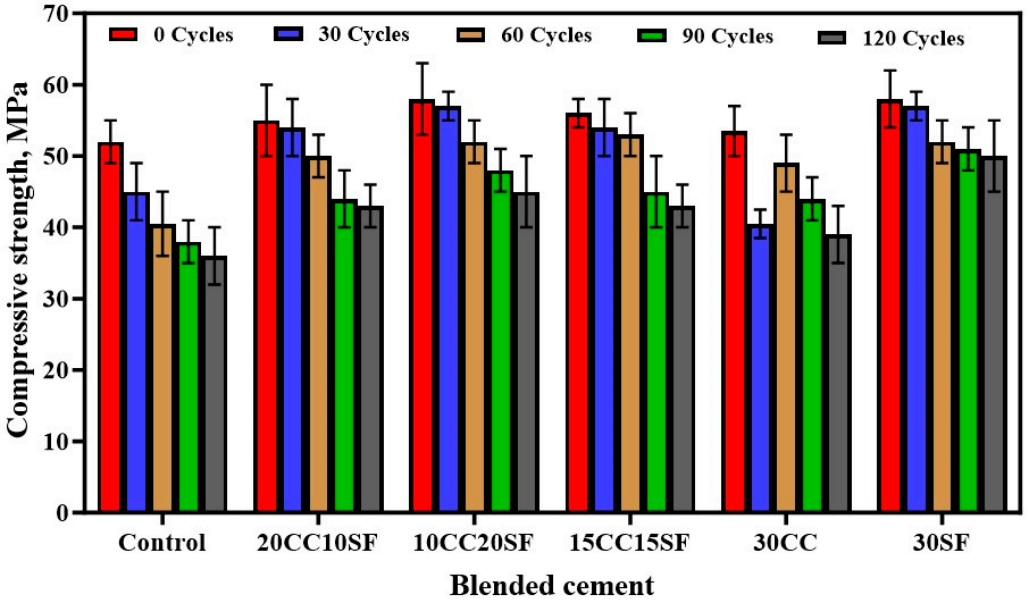


**Figure 11.** Effect of freeze–thaw cycles on blended cements.

Strength retention values for 20CC10SF, 10CC20SF, 15CC15SF, 30CC and 30SF were 79.6%, 77.6%, 76.8%, 72.9% and 86.2%. This implies that the best-performing blended cement mix (30SF) outperformed the least (Control) by 23%. The deterioration of cementitious materials by freeze and thaw occurs within the pore structure of the material via the release of expansive forces during the freezing of bound water. Thus, the amount of ice present

determines the severity of freeze–thaw damage, which is directly related to the porosity of the cementitious material [52]. Superior freeze and thaw resistance in the blended cement mixes is attributed to finer pore structure and lower porosity compared to the control mix. This leads to a relatively lower internal expansive force and a higher resistance to freeze and thaw attack. This explains the reason for the better freeze–thaw resistance in SF-rich samples. Similar trend of results was reported by earlier researchers [52–54].

#### 3.6.3. Drying Shrinkage

The contraction of the overall mass upon moisture loss causes shrinkage, a common phenomenon that affects practically all cementitious products. Figure 12 is a graphical presentation of the drying shrinkage results for the control and ternary blended cement mixes cured for 3, 7, 14, 28 and 91 days. Drying shrinkage was found to be more severe in the first 14 days of the curing. By 14 days, the samples had obtained about 75% of the total shrinkage recorded after 91 days of curing. This is about 10% of the total shrinkage of ordinary Portland cement which can record a potential drying shrinkage up to 1000 microstrain [55]. From Figure 13, drying shrinkage was found to be less severe in the control mortar than the blended cement mixes. Different blended cement mixes impacted drying shrinkage differently. Results recorded for 20CC10SF, 10CC20SF, 15CC15SF, 30CC and 30SF after 91 days curing were 31.54, 45.8, 33.45, 50.67 and 54.5 microstrain, respectively. Drying shrinkage in the blended cement mixes containing silica fume obtained higher values than the ones without. Rao [56], in his study on the long-term influence of silica fume, reported an increase of about 10% in drying shrinkage with the addition of silica fume. This was supported by studies conducted by Zang et al. [57]. Mortar mixes containing calcined clay outperformed silica fume-rich mixes in withstanding drying shrinkage. Increased drying shrinkage in silica fume blended mortars is due to pozzolanic reactivity and pore refinement mechanisms within the cementitious matrix [56,58].

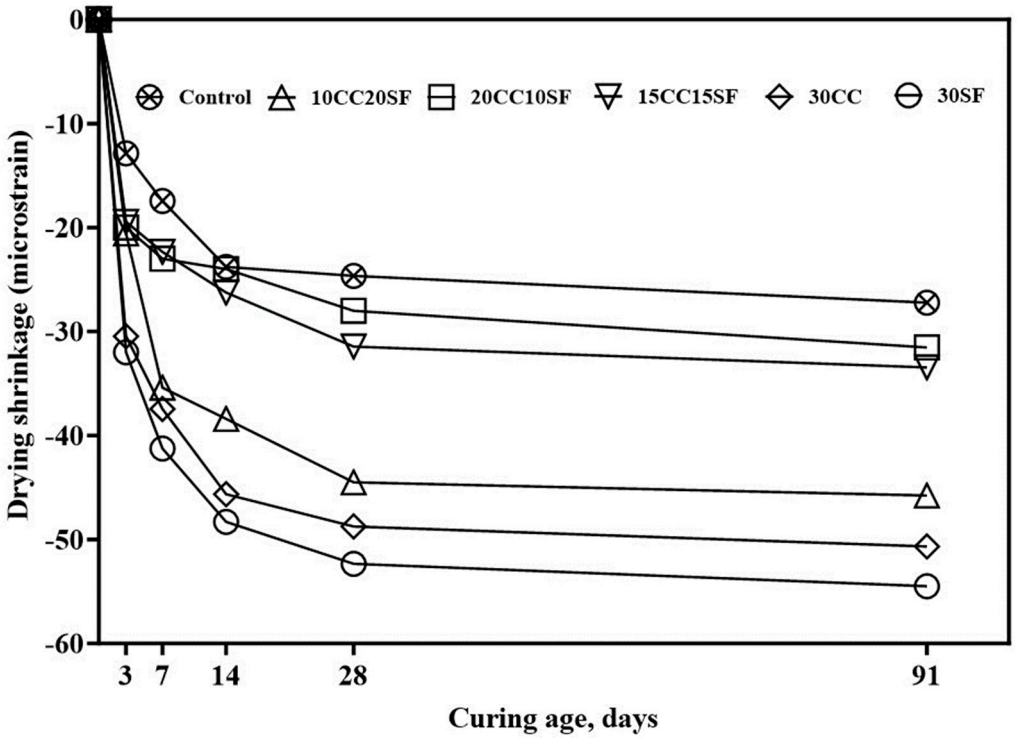


**Figure 12.** Drying shrinkage of ternary blended cement.

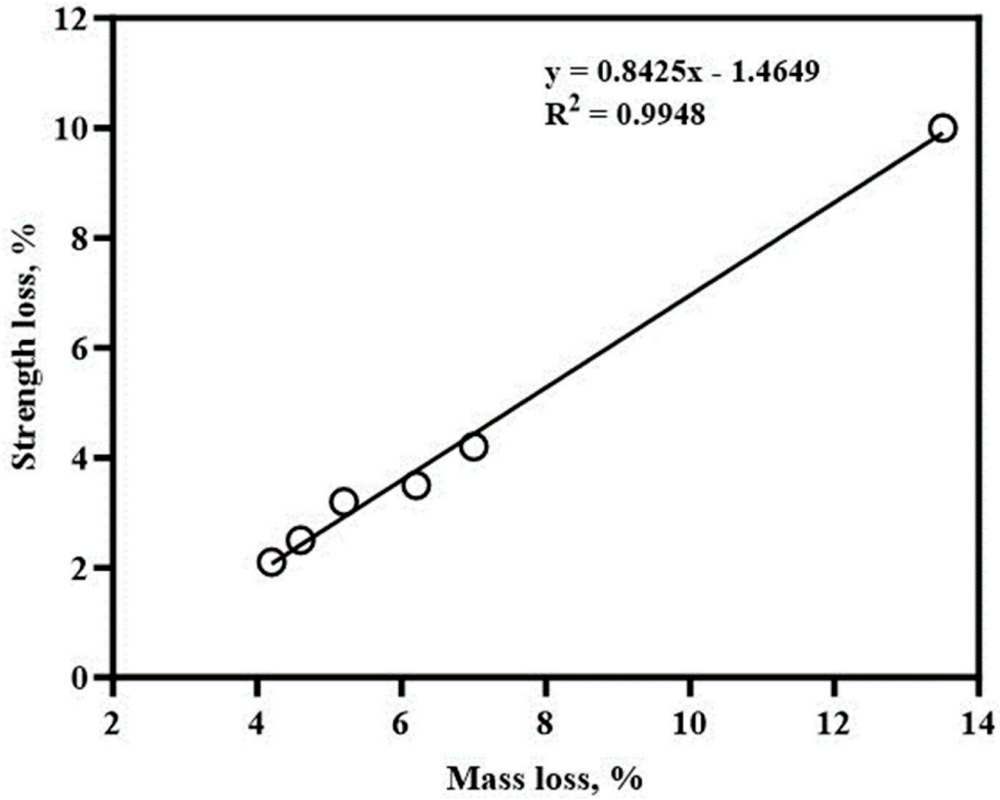


**Figure 13.** Relationship between mass loss and strength loss.

#### 3.6.4. Sulphate Resistance

The ability of mortar and concrete to resist sulphate attack is crucial to their service performance and durability. Table 4 presents the impact of 5%-$Na_2SO_4$ on compressive strength and weight after immersing the samples for 90 days. The relationship between mass loss and compressive strength is shown in Figure 13. The mass and compressive strength of the blended cement mortar is seen to be negatively impacted by 5% $Na_2SO_4$. When compared to the blended cement specimens, the control suffered the most weight (13.3%) and strength (10%) losses. An increase in silica fume content in the mix resulted in a corresponding decrease in weight and compressive strength. Samples marked 20CC10SF, 10CC20SF, 15CC15SF, 30CC and 30SF recorded 7%, 5.2%, 6.2%, 4.6% and 4.2% mass losses, and 4.2%, 3.2%, 3.5%, 2.5% and 2.1% compressive strength losses, respectively. Changes in mass and strength are caused by interactions between the hydrated cement and sulphate ions, leading to the secondary formation of ettringite and changes in phase assemblage which could ultimately result in expansion and mass and strength loss [59]. Relatively lower effect of sulphate attack on the blended cement specimens is due to refinement of the pore structure and depreciation of tricalcium aluminate ($C_3A$) in the mix [59]. This leads to an increasing consumption of excess $Ca(OH)_2$ through the pozzolanic reactivity of the mineral admixtures. From the results, it can be seen that pozzolanic reactions in the silica fume-rich specimens were more effective compared to that of calcined clay. As seen in the relationship between mass loss and strength loss in Figure 13, compressive strength decreased with increasing mass loss. An $R^2$ value of 0.9948 was obtained which indicates a good fit.

**Table 4.** Changes in mass and compressive strength.

| Sample | Mass Loss, % | Strength Loss, % |
|---|---|---|
| Control | 13.5 | 10 |
| 30CC | 7.0 | 4.2 |
| 20CC10SF | 5.2 | 3.2 |
| 15CC15SF | 6.2 | 3.5 |
| 10CC20SF | 4.2 | 2.1 |
| 30SF | 4.6 | 2.5 |

## 4. Conclusions

This study has investigated the use of binary and ternary blended calcined clay and silica fume as alternative binder, and their effect on hydration, reactivity and the mechanical and durability properties of cementitious mortar. Overall, the experimental findings showed that the co-addition of calcined clay and silica fume can improve the fresh and hardened properties of mortar by harnessing the individual characteristics of the pozzolans involved. The following conclusions have been drawn from analysis of the results:

1. After 28 days of hydration, XRD analysis revealed substantially smaller peaks in the blended cement pastes. This is attributed to the reaction between the calcined clay/silica fume and portlandite to generate additional cementitious products like calcium silicate hydrates, evidenced by the improvement of strength in the ternary mixtures, especially at later ages.
2. The portlandite consumption test showed a significant depletion of $Ca(OH)_2$ in the blended cement mixes compared to the control paste. Pastes containing a ternary blend of calcined clay and silica fume showed a relatively higher degree of pozzolanic reactivity, resulting in lower levels of portlandite after 91 days of hydration. Between the two pozzolans, silica fume-rich pastes were found to contain less portlandite content at the end of the curing period. This was confirmed by the Frattini test results.
3. Generally, all blended cement samples exhibited lower porosity and permeability compared to the control. Porosity in silica fume-rich samples was found to be inversely proportional to the degree of porosity and permeability. The higher the silica fume content, the lower the sorptivity coefficient. Even though all samples suffered a reduction in strength as a result of the freeze–thaw cycles, the blended cement samples, irrespective of pozzolan content and dosages, demonstrated a better resistance compared to the control mix. Among the blended cements, the paste prepared with 30% silica fume offered the greatest resistance to freeze and thaw.
4. Drying shrinkage was found to be less severe in the control mortar than the blended cement mixes. Different blended cement mixes impacted drying shrinkage differently. Drying shrinkage in the blended cement mixes containing silica fume was more pronounced than the ones without. A higher level of sulphate resistance was achieved in the calcined clay-silica fume composite cements than the control. Compared to the blended cement specimens, the control suffered the most weight (13.3%) and strength (10%) losses. An increase in silica fume content in the mix resulted in a corresponding decrease in weight and compressive strength.
5. Compressive strength of all the blended cement mortar mixes trailed behind the control mortar at 3 and 7 days. SF-rich ternary blended mixes were observed to outperform the CC-rich mixes at early ages. However, at 91 days, compressive strength significantly improved, outperforming the reference cement mortar.

The findings of this research are expected to contribute to the development and utilisation of alternative binders for infrastructure, especially in areas where conventions SCM's are scarce. The mix designs tested and presented in this research offer a wide range of options for construction applications depending on the intended purpose. Further studies into the long-term durability of these ternary mixes are recommended.

**Author Contributions:** Writing—original draft, K.B.; Supervision, M.K. All authors have read and agreed to the published version of the manuscript.

**Funding:** This research received no external funding, and The APC was funded by MDPI open access publishing in Basel/Switzerland.

**Institutional Review Board Statement:** Not applicable.

**Informed Consent Statement:** Not applicable.

**Data Availability Statement:** Not applicable.

**Conflicts of Interest:** The authors declare no conflict of interest.

## References

1. Juenger, M.C.G.; Snellings, R.; Bernal, S.A. Supplementary cementitious materials: New sources, characterization, and performance insights. *Cem. Concr. Res.* **2019**, *122*, 257–273. [CrossRef]
2. Senhadji, Y.; Escadeillas, G.; Mouli, M.; Khelafi, H.; Benosman. Influence of natural pozzolan, silica fume and limestone fine on strength, acid resistance and microstructure of mortar. *Powder Technol.* **2014**, *254*, 314–323. [CrossRef]
3. Boakye, K.; Khorami, M. Effect of calcined clay on fresh and hardened properties of self-compacting concrete (SCC). *Curr. Trends Civil. Struct. Eng.* **2023**, *9*, 1–9.
4. Cardinaud, G.; Rozière, E.; Martinage, O.; Loukili, A.; Barnes-Davin, L.; Paris, M.; Deneele, D. Calcined clay—Limestone cements: Hydration processes with high and low-grade kaolinite clays. *Constr. Build. Mater.* **2021**, *277*, 122271. [CrossRef]
5. Ferreiro, S.; Canut, M.M.C.; Lund, J.; Herfort, D. Influence of fineness of raw clay and calcination temperature on the performance of calcined clay-limestone blended cements. *Appl. Clay Sci.* **2019**, *169*, 81–90. [CrossRef]
6. Fernandez, R.; Martirena, F.; Scrivener, K.L. The origin of the pozzolanic activity of calcined clay minerals: A comparison between kaolinite, illite and montmorillonite. *Cem. Concr. Res.* **2011**, *41*, 113–122. [CrossRef]
7. Scrivener, K.; Martirena, F.; Bishnoi, S.; Maity, S. Calcined clay limestone cements (LC3). *Cem. Concr. Res.* **2018**, *114*, 49–56. [CrossRef]
8. Alujas, A.; Fernández, R.; Quintana, R.; Scrivener, K.L.; Martirena, F. Pozzolanic reactivity of low grade kaolinitic clays: Influence of calcination temperature and impact of calcination products on OPC hydration. *Appl. Clay Sci.* **2015**, *108*, 94–101. [CrossRef]
9. Zheng, D.; Liang, X.; Cui, H.; Tang, W.; Liu, W.; Zhou, D. Study of performances and microstructures of mortar with calcined low-grade clay. *Constr. Build. Mater.* **2022**, *327*, 126963. [CrossRef]
10. Zhou, D.; Wang, R.; Tyrer, M.; Wong, H.; Cheeseman, C. Sustainable infrastructure development through use of calcined excavated waste clay as a supplementary cementitious material. *J. Clean. Prod.* **2017**, *168*, 1180–1192. [CrossRef]
11. Du, H.; Pang, S.D. Value-added utilization of marine clay as cement replacement for sustainable concrete production. *J. Clean. Prod.* **2018**, *198*, 867–873. [CrossRef]
12. Ding, J.; Li, Z. Effects of metakaolin and silica fume on properties of concrete. *Mater. J.* **2002**, *99*, 393–398.
13. Ramezanianpour, A.A.; Malhotra, V.M. Effect of curing on the compressive strength, resistance to chloride-ion penetration and porosity of concretes incorporating slag, fly ash or silica fume. *Cem. Concr. Compos.* **1995**, *17*, 125–133. [CrossRef]
14. Khan, M.I.; Siddique, R. Utilization of silica fume in concrete: Review of durability properties. *Resour. Conserv. Recycl.* **2011**, *57*, 30–35. [CrossRef]
15. Wu, Z.; Shi, C.; Khayat, K.H. Influence of silica fume content on microstructure development and bond to steel fiber in ultra-high strength cement-based materials (UHSC). *Cem. Concr. Compos.* **2016**, *71*, 97–109. [CrossRef]
16. Alexander, M.G.; Magee, B.J. Durability performance of concrete containing condensed silica fume. *Cem. Concr. Res.* **1999**, *29*, 917–922. [CrossRef]
17. Chu, S.H.; Kwan, A.K.H. Co-addition of metakaolin and silica fume in mortar: Effects and advantages. *Constr. Build. Mater.* **2019**, *197*, 716–724. [CrossRef]
18. Boakye, K.; Khorami, M. Influence of Calcined Clay Pozzolan and Aggregate Size on the Mechanical and Durability Properties of Pervious Concrete. *J. Compos. Sci.* **2023**, *7*, 182. [CrossRef]
19. Boakye, K.; Khorami, M.; Saidani, M.; Ganjian, E.; Dunster, A.; Ehsani, A.; Tyrer, M. Mechanochemical characterisation of calcined impure kaolinitic clay as a composite binder in cementitious mortars. *J. Compos. Sci.* **2022**, *6*, 134. [CrossRef]
20. Padavala, A.B.; Potharaju, M.; Kode, V.R. Mechanical properties of ternary blended mix concrete of fly ash and silica fume. *Mater. Today Proc.* **2021**, *43*, 2198–2202. [CrossRef]
21. Boakye, K.; Khorami, M. Impact of low-reactivity calcined clay on the performance of fly ash-based geopolymer mortar. *Sustainability* **2023**, *15*, 13556. [CrossRef]
22. Morsy, M.M.; Shebl, S.S.; Rashad, A.M. Effect of fire on microstructure and mechanical properties of blended cement pastes containing metakaolin and silica fume. In Proceedings of the 11DBMC International Conference on Durability of Building Materials and Components, Istanbul, Turkey, 11–14 May 2008.
23. Benkeser, D.; Hernandez, K.; Lolli, F.; Kurtis, K. Influence of calcined clay morphology on flow in blended cementitious systems. *Cem. Concr. Res.* **2022**, *160*, 106927. [CrossRef]

24. *ASTM C305-20*; Standard Practice for Mechanical Mixing of Hydraulic Cement Pastes and Mortars of Plastic Consistency. American Society for Testing and Materials: West Conshohocken, PA, USA, 1995.
25. *ASTM C1437-20*; Standard Test Method for Flow of Hydraulic Cement Mortar. American Society for Testing and Materials: West Conshohocken, PA, USA, 2007.
26. *ASTM C191-21*; Standard Test Methods for Time of Setting of Hydraulic Cement by Vicat Needle. ASTM International: West Conshohocken, PA, USA, 2013.
27. *BS EN 196-3:1995*; Methods of Testing Cement-Part 3: Determination of Setting Time and Soundness. British Standards Institute: London, UK, 1999.
28. *EN BS 196-5*; Methods of Testing Cement, Pozzolanicity Test for Pozzolanic Cement. British Standards Institution: London, UK, 2011.
29. *ASTM C1585-20*; Standard Test Method for Measurement of Rate of Absorption of Water by Hydraulic-Cement Concretes. ASTM International: West Conshohocken, PA, USA, 2020.
30. *ASTM C642*; Standard Test Method for Density, Absorption, and Voids in Hardened Concrete. ASTM International: West Conshohocken, PA, USA, 2013.
31. *ASTM C490-07*; Standard Test Method Standard Practice for Use of Apparatus for the Determination of Length Change of Hardened Cement Paste, Mortar, and Concrete. American Society for Testing and Materials: West Conshohocken, PA, USA, 2010.
32. *ASTM C1202-19*; Standard Test Method for Electrical Indication of Concrete's Ability to Resist Chloride Ion Penetration. ASTM International: West Conshohocken, PA, USA, 1997.
33. Rao, G.A. Investigations on the performance of silica fume-incorporated cement pastes and mortars. *Cem. Concr. Res.* **2003**, *33*, 1765–1770. [CrossRef]
34. Tang, Y.; Zhao, L.; Li, B.; Chen, W. Controlling the soundness of Portland cement clinker synthesized with solid wastes based on phase transition of $MgNiO_2$. *Cem. Concr. Res.* **2022**, *157*, 106832. [CrossRef]
35. Boakye, K.; Khorami, M. Mechanical and durability performance of ternary blended calcined clay and pulverized granite mortar composites. In *Advances in Materials and Processing Technologies*; Taylor & Francis: Abingdon, UK, 2023; pp. 1–20.
36. Hu, L.; He, Z. A fresh perspective on effect of metakaolin and limestone powder on sulfate resistance of cement-based materials. *Constr. Build. Mater.* **2020**, *262*, 119847. [CrossRef]
37. Bentz, D.P.; Ferraris, C.F.; Jones, S.Z.; Lootens, D.; Zunino, F. Limestone and silica powder replacements for cement: Early-age performance. *Cem. Concr. Compos.* **2017**, *78*, 43–56. [CrossRef]
38. Beaudoin, J.; Odler, I. 5—Hydration, Setting and Hardening of Portland Cement. In *Lea's Chemistry of Cement and Concrete*, 5th ed.; Hewlett, P.C., Liska, M., Eds.; Butterworth-Heinemann: Oxford, UK, 2019; pp. 157–250.
39. Kumar, M.; Singh, S.K.; Singh, N.P. Heat evolution during the hydration of Portland cement in the presence of fly ash, calcium hydroxide and super plasticizer. *Thermochim. Acta* **2012**, *548*, 27–32. [CrossRef]
40. Ramanathan, S.; Moon, H.; Croly, M.; Chung, C.; Suraneni, P. Predicting the degree of reaction of supplementary cementitious materials in cementitious pastes using a pozzolanic test. *Constr. Build. Mater.* **2019**, *204*, 621–630. [CrossRef]
41. Sarfo-Ansah, J.; Atiemo, E.; Boakye, K.; Adjei, D.; Adjaottor, A. Calcined Clay Pozzolan as an Admixture to Mitigate the Alkali-Silica Reaction in Concrete. *J. Mater. Sci. Chem. Eng.* **2014**, *2*, 20–26. [CrossRef]
42. Wild, S.; Khatib, J.M. Portlandite consumption in metakaolin cement pastes and mortars. *Cem. Concr. Res.* **1997**, *27*, 137–146. [CrossRef]
43. Taylor-Lange, S.C.; Lamon, E.L.; Riding, K.A.; Juenger, M.C.G. Calcined kaolinite–bentonite clay blends as supplementary cementitious materials. *Appl. Clay Sci.* **2015**, *108*, 84–93. [CrossRef]
44. Jensen, O.M. The pozzolanic reaction of silica fume. *MRS Online Proc. Libr.* **2012**, *1488*, 43–54. [CrossRef]
45. Hollanders, S.; Adriaens, R.; Skibsted, J.; Cizer, Ö.; Elsen, J. Pozzolanic reactivity of pure calcined clays. *Appl. Clay Sci.* **2016**, *132–133*, 552–560. [CrossRef]
46. Donatello, S.; Tyrer, M.; Cheeseman, C.R. Comparison of test methods to assess pozzolanic activity. *Cem. Concr. Compos.* **2010**, *32*, 121–127. [CrossRef]
47. Seeni, B.S.; Madasamy, M.; Chellapandian, M.; Arunachelam, N. Effect of silica fume on the physical, hydrological and mechanical properties of pervious concrete. *Mater. Today Proc.* 2023; *in press*. [CrossRef]
48. Hamada, H.M.; Abed, F.; Binti Katman, H.Y.; Humada, A.M.; Al Jawahery, M.S.; Majdi, A.; Yousif, S.T.; Thomas, B.S. Effect of silica fume on the properties of sustainable cement concrete. *J. Mater. Res. Technol.* **2023**, *24*, 8887–8908. [CrossRef]
49. Weng, J.K.; Langan, B.W.; Ward, M.A. Pozzolanic reaction in Portland cement, silica fume, and fly ash mixtures. *Can. J. Civ. Eng.* **1997**, *24*, 754–760. [CrossRef]
50. Richard Liew, J.Y.; Xiong, M.; Lai, B. Chapter 07—Special considerations for high strength materials. In *Design of Steel-Concrete Composite Structures Using High-Strength Materials*; Richard Liew, J.Y., Xiong, M., Lai, B., Eds.; Woodhead Publishing: Sawston, UK, 2021; pp. 125–142.
51. Chen, J.J.; Ng, P.L.; Chu, S.H.; Guan, G.X.; Kwan, A.K.H. Ternary blending with metakaolin and silica fume to improve packing density and performance of binder paste. *Constr. Build. Mater.* **2020**, *252*, 119031. [CrossRef]
52. Qin, Z.; Ma, C.; Zheng, Z.; Long, G.; Chen, B. Effects of metakaolin on properties and microstructure of magnesium phosphate cement. *Constr. Build. Mater.* **2020**, *234*, 117353. [CrossRef]
53. Kalkan, E. Effects of silica fume on the geotechnical properties of fine-grained soils exposed to freeze and thaw. *Cold Reg. Sci. Technol.* **2009**, *58*, 130–135. [CrossRef]

54. Sabir, B.B. Mechanical properties and frost resistance of silica fume concrete. *Cem. Concr. Compos.* **1997**, *19*, 285–294. [CrossRef]
55. Formosa, J.; Lacasta, A.M.; Navarro, A.; del Valle-Zermeño, R.; Niubó, M.; Rosell, J.R.; Chimenos, J. Magnesium Phosphate Cements formulated with a low-grade MgO by-product: Physico-mechanical and durability aspects. *Constr. Build. Mater.* **2015**, *91*, 150–157. [CrossRef]
56. Rao, G.A. Long-term drying shrinkage of mortar—Influence of silica fume and size of fine aggregate. *Cem. Concr. Res.* **2001**, *31*, 171–175. [CrossRef]
57. Zhang, P.; Li, Q. Durability of high performance concrete composites containing silica fume. *Proc. Inst. Mech. Eng. Part L J. Mater. Des. Appl.* **2013**, *227*, 343–349. [CrossRef]
58. Buil, M.; Paillère, A.M.; Roussel, B. High strength mortars containing condensed silica fume. *Cem. Concr. Res.* **1984**, *14*, 693–704. [CrossRef]
59. Shi, Z.; Ferreiro, S.; Lothenbach, B.; Geiker, M.R.; Kunther, W.; Kaufmann, J.; Herfort, D.; Skibsted, J. Sulfate resistance of calcined clay—Limestone—Portland cements. *Cem. Concr. Res.* **2019**, *116*, 238–251. [CrossRef]